European Journal of Chemistry 14 (1) (2023) 53-64

European Journal of **Chem**istry

View Journal Online
View Article Online

Spectroscopic study of solvent effects on the electronic absorption spectra of morpholine and its complexes

Mamdouh Saad Masoud [1], Alaa Eldin Ali [2],
Gehan Shaaban Elasala [2] and Rehab Elsaid Elwardany [2,*]

[1] *Department of Chemistry, Faculty of Science, University of Alexandria, Alexandria, 21515, Egypt*
[2] *Department of Chemistry, Faculty of Science, University of Damanhour, Damanhour, 22511, Egypt*

* *Corresponding author at: Department of Chemistry, Faculty of Science, University of Damanhour, Damanhour, 22511, Egypt.*
e-mail: rehabelwardany@sci.dmu.edu.eg (R.E. Elwardany).

RESEARCH ARTICLE

10.5155/eurjchem.14.1.53-64.2365

Received: 25 November 2022
Received in revised form: 05 January 2023
Accepted: 14 January 2023
Published online: 31 March 2023
Printed: 31 March 2023

KEYWORDS
UV spectra
Absorption
Dipole moment
Solvent polarity
Solvatochromic
Morpholine complexes

ABSTRACT

The electronic absorption spectra of morpholine and its five morpholine complexes have been studied in different solvents of various polarities. The regression and correlation coefficients have been calculated with the SPSS program. Solvation energy relationships were deduced from spectral shifts and correlated with solvent parameters α (solvent hydrogen bond donor acidity), β (solvent hydrogen bond acceptor basicity), and π* (dipolarity/polarizability). The percentage contributions of the calculated solvatochromic parameters show that classic solvation effects play a major role in explaining the spectral shifts in all investigated complexes. The blue shift of $[Fe(MOR)_3Cl_3]\cdot 4H_2O$, $[Ni(MOR)_4Cl_2]\cdot 4H_2O$, and $[Cu(MOR)_4Cl_2]\cdot 6H_2O$ complexes is due to the formation of hydrogen bonds, which suggests the stabilization of the ground electronic state compared with the excited state. $[CuNi(MOR)_2Cl_4]\cdot 4H_2O$ and $[CuZn(MOR)_3Cl_4]\cdot 2H_2O$ are mixed metal complexes that suffer a red shift due to the solute-solvent interactions, which causes stabilization of the excited solute state with increasing solvent polarity. The bands are affected by specific solute-solvent interactions including hydrogen bond donor ability (acidity) and hydrogen bond acceptor ability (basicity) and nonspecific solute-solvent interactions including electromagnetic interaction between the dipole moments of solute and polar solvents.

Cite this: *Eur. J. Chem.* **2023**, *14(1)*, 53-64 **Journal website**: www.eurjchem.com

1. Introduction

Morpholine is an organic compound with ether-like properties due to the presence of an oxygen atom and amine-like properties due to the presence of a nitrogen atom (Figure 1). Many molecules derived from morpholines have very good biological activity in different therapeutic areas, such as antiviral, antibacterial, anticancer, antidiabetic, antimicrobial, antimalarial, inflammatory, and antifungal activities [1,2]. The most important applications of complexes are drugs; therefore, they must dissolve in the proper solvent. For the development of solution chemistry, it is essential to study the structure and spectroscopic behavior of a solute in different solvents [3-7].

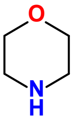

Figure 1. Structure of morpholine (MOR).

Solvatochromism is a phenomenon that describes the effect of using different solvents with varying polarities on the UV-visible absorption spectra of a chemical compound [8,9]. The interaction between solvents and a solute was classified into nonspecific interactions, including electromagnetic interactions between the dipole moments of the solute and a polar solvent, and specific interactions including the ability of hydrogen bond donors (acidity) and the ability of hydrogen bond acceptors (basicity) [10]. The presence of specific and nonspecific interactions between the solvent and solute molecules is responsible for the change in the molecular geometry, electronic structure, and dipolar moment of the solute. Empirical parameters of solvent polarity have been developed to interpret and substantiate the solute-solvent interaction using spectroscopic data. The effect of solvent on UV-visible spectra can be shown by a change in the position, intensity, and shape of the absorption bands [11]. The change in the position of bands with increasing solvent polarity can be described in two ways. The first is the hypsochromic shift (blue shift) to a negative Δλ (nm), and the second is the bathochromic shift (red shift) with a positive Δλ (nm). Solvatochromism is caused by differential solvation of the ground and first excited states of the light absorption molecule (chromophore). With increasing solvent polarity, better stabilization of the molecule in the ground state than in the excited state leads to negative

ISSN 2153-2249 (Print) / ISSN 2153-2257 (Online)
https://dx.doi.org/10.5155/eurjchem.14.1.53-64.2365

Table 1. Analytical data and physical properties of morpholine complexes.

Compound	Molecular formula	M.wt. (g/mol)	Color	Found (Calculated) (%)		
				M		Cl
[Fe(MOR)$_3$Cl$_3$]·4H$_2$O (1:3)	$C_{12}H_{35}N_3O_7Cl_3Fe$	495.65	Brown	Fe 11.20 (11.30)		21.30 (21.45)
[Ni(MOR)$_4$Cl$_2$]·4H$_2$O (1:4)	$C_{16}H_{44}N_4O_8Cl_2Ni$	550.07	Pale green	Ni 10.94 (10.67)		12.49 (12.89)
[Cu(MOR)$_4$Cl$_2$]·6H$_2$O (1:4)	$C_{16}H_{48}N_4O_{10}C_{l2}Cu$	590.92	Green	Cu 10.90 (10.75)		12.25 (11.99)
[CuZn(MOR)$_3$Cl$_4$]·2H$_2$O (1:1:3)	$C_{12}H_{31}N_3O_5Cl_4CuZn$	568.11	Pale green	Cu 11.40 (11.18)	Zn 11.29 (11.51)	25.20 (24.96)
[CuNi(MOR)$_2$Cl$_4$]·4H$_2$O (1:1:2)	$C_8H_{26}N_2O_6Cl_4CuNi$	510.27	Green	Cu 12.10 (12.45)	Ni 11.71 (11.50)	27.95 (27.79)

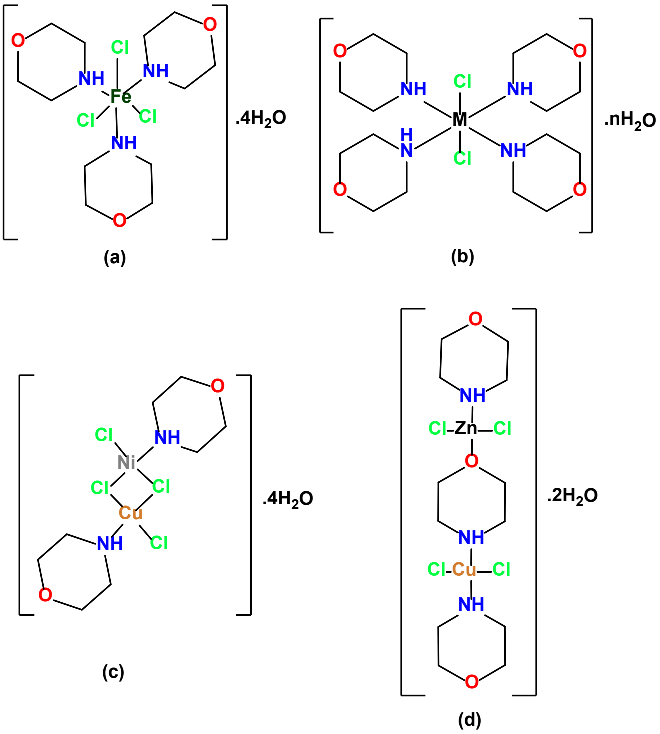

Figure 2. Suggested structures of morpholine metal complexes (a) [Fe(MOR)$_3$Cl$_3$]·4H$_2$O, (b) [M(MOR)$_4$Cl$_2$].nH$_2$O M(n) = Ni(4), Cu(6), (c) [CuNi(MOR)$_2$Cl$_4$]·4H$_2$O, and (d) [CuZn(MOR)$_3$Cl$_4$]·2H$_2$O.

solvatochromism. On the other hand, better stabilization of the molecule in the first excited state compared to that in the ground state leads to positive solvatochromism. These shifts are due to the solvent stabilization of the excited or ground electronic states, thus resulting in a change in the energy gap between the energy levels involved in the transition. The represented electronic absorption spectra of the compounds in the presence of different solvents of different polarities had a wide variety of solvent parameters, causing a change in the intensity and position of the bands. This change is due to the polarity of the solvent, London-dispersion forces between the nonpolar solute and nonpolar solvent, and the difference in the solvation energy from one solvent to another. In this work, morpholine (MOR) and its five morpholine complexes were dissolved in different solvents of various polarities, and the electronic absorption spectra were studied to investigate the effect of solvents on the electronic transition.

2. Experimental

2.1. Preparation of morpholine complexes

Simple metal morpholine complexes were prepared in a similar manner [12]. Inorganic salts Fe(III), Ni(II), and Cu(II) were dissolved as chlorides in 10 mL of bidistilled water. Excess liquid morpholine (MOR) was added (50 mL) and the resulting solid complexes were removed by filtration. Then they were washed several times with a mixture of ethanol and water and dried under a desiccator over anhydrous CaCl$_2$. Two mixed-metal complexes of morpholine were prepared. 0.5 g of each metal chloride in 10 mL of water, then mix the two solutions. Excess liquid morpholine was added while stirring. The precipitated complexes were separated by filtration, then washed with an ethanol:water mixture, and dried in a vacuum desiccator over anhydrous CaCl$_2$.

2.2. Characterization of the prepared complexes

The metal contents were determined according to the atomic absorption technique using the Shimadzu 6650 model atomic absorption spectrophotometer [13] and complex-metric titration with EDTA solution [14]. The chloride content of the complexes was determined using the well-known Volhard method [15]. The IR spectra of the ligand and its metal complexes were recorded using the potassium bromide disc technique in the range 400-4000 cm^{-1} using a Perkin-Elmer 1430 spectrophotometer. The electron spin resonance (ESR) spectra of the copper complexes were recorded with a reflection spectrometer operating at 8.7 GHz (X-band) in a cylindrical resonance cavity with 100 kHz modulation at the Central Lab of The Faculty of Science at Alexandria University, Alexandria, Egypt. At room temperature, molar magnetic susceptibilities were measured using the Faraday's method and corrected for diamagnetism using Pascal's constants [16]. Hg[Co(SCN)$_4$] was used to calibrate the apparatus. A Perkin Elmer spectrophotometer, model Lambda 4B, was used for UV-vis spectra, covering the wavelength range 200-800 nm. The analytical results are given in Table 1, depicting the formation of complexes with different stoichiometries (Figure 2).

Table 2. Fundamental infrared bands (cm^{-1}) of morpholine and its metal complexes.

Compound	ν_{NH}	$\nu_{C\text{-}O\text{-}C}$	νM-O	νM-N	νM-Cl
Morpholine	3313	1099	-	-	-
$[Fe(MOR)_3Cl_3]\cdot4H_2O$	3120	1101	-	487	437
$[Ni(MOR)_4Cl_2]\cdot4H_2O$	3280	1099	-	480	438
$[Cu(MOR)_4Cl_2]\cdot6H_2O$	3225	1109	-	450	420
$[CuZn(MOR)_3Cl_4]\cdot2H_2O$	3240	1089	600	503, 480	439, 405
$[CuNi(MOR)_2Cl_4]\cdot4H_2O$	3047	1104	-	460, 480	440, 416

Table 3. Electronic absorption spectra of morpholine (MOR) and its complexes in the presence of different solvents (λ_{max}, nm).

Compound	CCl_4	$CHCl_3$	*i*-propanol	Acetone	Ethanol	Methanol	Water	$\Delta\lambda$ (nm)
Morpholine	200	202	203	204	205	206	207	+7
	225	230	231	235	236	-	230	+11
$[Fe(MOR)_3Cl_3]\cdot4H_2O$	256	253	247	242	238	237	234	-22
	282	281	280	278	276	275	274	-8
$[Ni(MOR)_4Cl_2]\cdot4H_2O$	244	230	228	226	228	225	223	-21
	280	273	270	267	271	260	260	-20
$[Cu(MOR)_4Cl_2]\cdot6H_2O$	230	229	221	219	218	217	-	-13
	250	246	239	236	235	231	223	-27
$[CuNi(MOR)_2Cl_4]\cdot4H_2O$	230	231	232	232	234	234	236	+6
	293	305	305	307	308	309	310	+17
$[CuZn(MOR)_3Cl_4]\cdot2H_2O$	232	224	224	230	236	236	256	+24
	253.5	249	251	258	262	265	-	+11.5

2.3. Effect of solvents on UV-visible spectra of morpholine and its complexes

Morpholine spectral parameters and electronic absorption spectra, $[Fe(MOR)_3Cl_3]\cdot4H_2O$, $[Ni(MOR)_4Cl_2]\cdot4H_2O$, $[Cu(MOR)_4Cl_2]\cdot6H_2O$, $[CuZn(MOR)_3Cl_4]\cdot2H_2O$, $[CuNi(MOR)_2Cl_4]\cdot4H_2O$ complexes were analysed in the presence of seven solvents of varied polarities, namely water, methanol, ethanol, acetone, *i*-propanol, chloroform and carbon tetrachloride, which are all from Sigma Aldrich, USA Company. Spectrophotometric measurements in the visible and ultraviolet regions were recorded using a Perkin-Elmer spectrophotometer, model Lambda 4B, which covers the wavelength range 190-800 nm.

3. Results and discussion

3.1. IR, electronic spectra, ESR, and magnetic susceptibility of morpholine and its metal complexes

For liquid morpholine, the N-H stretching vibration occurs at 3313 cm^{-1} and the C-O-C stretching vibration is located at 1099 cm^{-1} [17]. For morpholine metal complexes, the N-H stretching vibration shifted to a lower frequency than that in the uncoordinated morpholine, due to the coordination of the metal ions. Morpholine acts as a monodentate ligand through the nitrogen atom only in all complexes except the $[CuZn(MOR)_3Cl_4]\cdot2H_2O$ complex. The shift of the C-O-C band, Table 2, supports the complexation through an oxygen atom and the formation of a morpholine bridge between the two metal ions, so morpholine acts as a bidentate ligand in this case [18].

The brown iron complex $[Fe(MOR)_3Cl_3]\cdot4H_2O$ has an electronic absorption spectrum that gives bands at 272, 347, and 434 nm, due to CT ($t_{2g} \rightarrow \pi^*$) and *d-d* transitions. Its room temperature μ_{eff} value of 5.95 B.M. typified the existence of an octahedral configuration. $[Ni(MOR)_4Cl_2]\cdot4H_2O$ is a pale green complex. The UV-visible spectra at 261, 352, 466, and 731 nm that are related to the transition from $^3A_{2g}$ as ground state to $^3T_{2g}(F)$, $^3T_{1g}(F)$ and $^3T_{1g}(P)$ according to the orgel diagram [19]. These transitions support the appearance of an octahedral geometry. The fact that the magnetic moment was 3.36 B.M. may be taken as additional evidence for its octahedral structure. $[Cu(MOR)_4Cl_2]\cdot6H_2O$ is a pale green complex gave two bands at 277 and 449 nm assigned to the transition $^2E_g \rightarrow {}^2T_{2g}(D)$ that can be assigned to the octahedral environment [20]. The room-temperature magnetic moment value is 2.84 B.M., which is higher than the value corresponding to one unpaired electron 1.73 B.M. due to the orbital contribution to the spin of the complexes. The pale green $[CuZn(MOR)_3Cl_4]\cdot2H_2O$ compound. Since the ESR data identified the perfect tetrahedral geometry around the Cu(II) ion, the complex showed five bands at 350, 409, 539, 556, and 625 nm [21]. The visible *d-d* electronic transition spectral band at 409 nm may be due to the tetrahedral configuration around Cu(II), and the weak bands at 539 and 556 nm may be due to the tetrahedral configuration around Zn(II) ions, also. The magnetic moment value is 2.15 B.M. and can be taken as additional evidence for its tetrahedral structure [22]. The pale green $[CuNi(MOR)_2Cl_4]\cdot4H_2O$ nujol mull electronic spectrum complex gave bands at 265, 354, and 503 nm since the ESR data identified the tetrahedral geometry around the Cu(II) ion. Thus, the visible *d-d* electronic spectral band at 503 nm may probably be due to the square planner configuration around the Ni(II) ion [23]. The complex has a magnetic field of 4.92 M.B. at room temperature. The ESR of the pale green complexes $[Cu(MOR)_4Cl_2]\cdot6H_2O$ at room temperature, $[CuZn(MOR)_3Cl_4]\cdot2H_2O$ and $[CuNi(MOR)_2Cl_4]\cdot4H_2O$, are near a similar pattern; all showed spectra with isotropic features where $g_s = 2.004$ with coupling constants A = 122.50, 80.00, and 70.00 ($\times10^{-4}$ cm^{-1}), respectively, which assign the presence of these three complexes in perfect octahedral or perfect tetrahedral structure [24].

3.2. Electronic absorption spectra

Representative UV-vis absorption spectra of morpholine (Figure 3a, Table 3) in a dilute solution (*ca*. 5×10^{-3} M), the absorption spectra exhibit two bands with maxima around 205 and 230 nm. The first band showed a strong nature, indicating the character of $\delta \rightarrow \delta^*$ transition, and the second band with a longer wavelength has a weak nature related to the $n \rightarrow \delta^*$ transition of the nitrogen or oxygen atom in the morpholine skeleton [25]. With increasing solvent polarity, the two bands showed a positive (red) bathochromic shift with stabilization of the solute excited state rather than the ground state. This suggests that this compound is more polar in the excited state than in the ground state. The red shift can also be explained by the hydrogen donor ability of the compound and the hydrogen acceptor nature of some solvents [26].

$[Fe(MOR)_3Cl_3]\cdot4H_2O$ for simple complexes and $[Cu(MOR)_4Cl_2]\cdot6H_2O$ as examples showed two bands allowed (Figure 3b, Table 3), in all solvents studied except water, in the case of $[Cu(MOR)_4Cl_2]\cdot6H_2O$ due to hydrolysis, only one band appeared. All simple complexes have a negative (blue) hypochromic shift (obtained from the wavenumber maximum absorption of the band recorded in the presence of the most polar solvent subtracted from that determined in the most nonpolar solvent

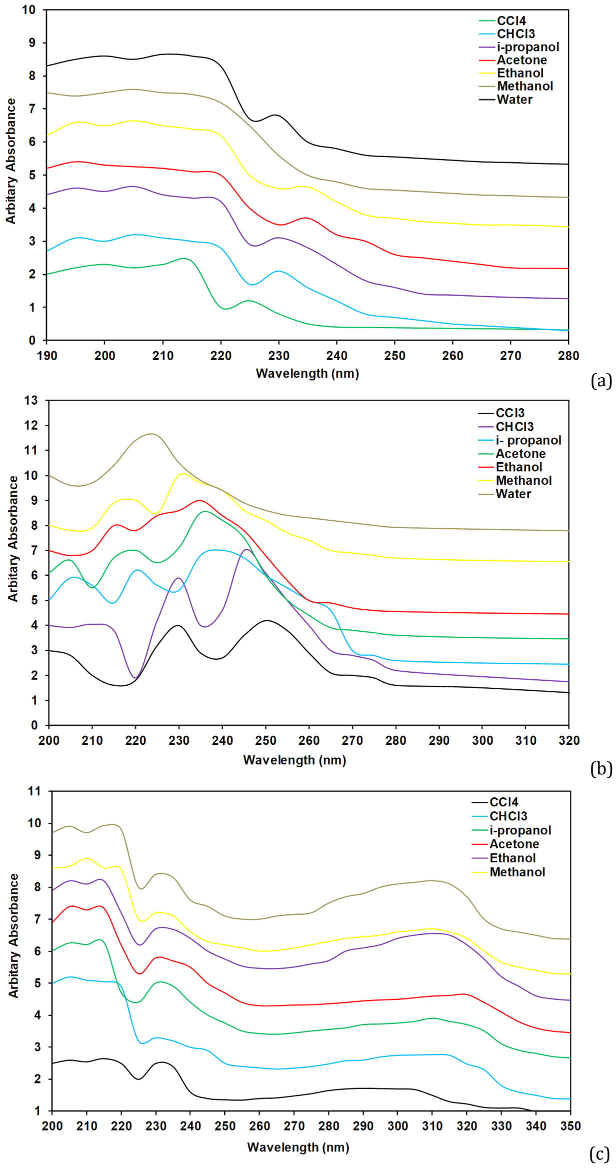

Figure 3. Effect of solvents on the electronic absorption spectra of a) morpholine, b) [Cu(MOR)$_4$Cl$_2$]·6H$_2$O complex, and c) [CuNi(MOR)$_2$Cl$_4$]·4H$_2$O complex.

Δλ nm), due to the formation of a hydrogen bond, and so the ground electronic state is more stabilized compared with the excited state. The first band in the range 230-260 nm is mainly of high energy bands of n → δ* type and the second band in the range 250-280 nm is due to the low-lying *d-d* electronic transition [27] that arose from the complexation with the copper ion, which is indicated by its absence in Figure 3. For the mixed metal complexes, [CuNi(MOR)$_2$Cl$_4$]·4H$_2$O and [CuZn (MOR)$_3$Cl$_4$]·2H$_2$O, as an example (Figure 3c, Table 3), two bands appeared in the UV-visible spectra with the use of different solvents, except water in the case of [CuZn(MOR)$_3$Cl$_4$]·2H$_2$O only one band appeared due to complete hydrolysis. The two complexes suffer a positive (red) bathochromic shift due to the solute-solvent interactions, causing stabilization of the excited solute state with increasing solvent polarity. This suggested that these complexes are more polar in the excited state than in the ground state [28]. The redshift can also be explained by the hydrogen donor ability of these complexes and the hydrogen acceptor nature of some solvents. The bands of low wavelength are mainly related to the n → δ* transition, and the bands of high wavelength are due to the *d-d* electronic transition absence in Figure 3a.

3.3. Application of the SPSS program and regression analysis

Multiple linear regression techniques were used to analyze the effects of the solvent on the electronic absorption spectra of morpholine and its complexes using the following equation:

$$y = a_0 + a_1x_1 + a_2x_2 + a_3x_3 + \ldots + a_nx_n \qquad (1)$$

where y is the observed peak location of an absorption band in a given solvent (wavelength), a_0 is the regression intercept. It has been assumed [29] to estimate the peak position for the gas phase spectra. a_1, a_2, ..., a_n are coefficients that could be determined by multiple regression techniques. x_1, x_2, ..., x_n are various empirical solvent polarity parameters calculated from the following relations.

$$E = 2.859\times10^{-3}\,\nu_{max} \qquad (2)$$

$$M = \frac{n^2-1}{2n^2+1} \qquad (3)$$

Table 4. Solvent parameters for solvents *.

Solvent	n	D	E	M	N	K
CCl_4	1.460	2.2	32.5	0.215	0.012	0.222
$CHCl_3$	1.446	4.7	39.1	0.210	0.290	0.360
i-Propanol	1.377	18.3	48.6	0.187	0.622	0.460
Acetone	1.359	20.7	42.2	0.180	0.650	0.460
Ethanol	1.361	24.3	51.9	0.181	0.665	0.470
Methanol	1.329	32.6	55.5	0.169	0.710	0.477
Water	1.333	78.5	63.1	0.171	0.757	0.491

* n: The refractive index; D: Dielectric constant; E: The empirical solvent polarity; M: Account for the solute permanent dipole-solvent induced dipole; N: Solute permanent dipole-solvent permanent dipole interaction and K: Kirkwood's dielectric function.

Table 5. Regression analysis data of morpholine (MOR) *.

Parameters	a_0	a_1	a_2	a_3	a_4	MCC	P
y = 200-207 nm							
E	193.420	0.219	-	-	-	0.900	0.001
M	227.348	-125.235	-	-	-	0.889	0.001
N	199.589	8.062	-	-	-	0.841	0.004
K	194.621	21.992	-	-	-	0.746	0.008
E, M	210.016	0.122	-63.748	-	-	0.953	0.002
E, N	195.284	0.143	3.367	-	-	0.937	0.004
E, K	193.046	0.159	7.765	-	-	0.929	0.005
M, N	222.244	-102.472	1.576	-	-	0.892	0.012
M, K	221.932	-105.427	4.049	-	-	0.893	0.011
N, K	206.239	18.062	-28.439	-	-	0.865	0.018
E, M, N	209.407	0.121	-60.951	0.215	-	0.953	0.017
E, M, K	208.507	0.120	-58.201	1.332	-	0.953	0.017
E, N, K	198.470	0.133	8.041	-12.414	-	0.941	0.024
M, N, K	232.291	-190.080	-17.988	39.866	-	0.902	0.051
E, M, N, K	219.123	0.121	-145.216	-18.533	38.222	0.962	0.075
y = 225-236 nm							
E	224.378	0.147	-	-	-	0.158	0.435
M	259.847	-150.424	-	-	-	0.542	0.144
N	225.958	10.430	-	-	-	0.570	0.083
K	218.802	30.121	-	-	-	0.610	0.067
E, M	298.955	-0.268	-290.635	-	-	0.584	0.268
E, N	235.943	-0.329	20.918	-	-	0.788	0.097
E, K	221.892	-0.283	54.501	-	-	0.799	0.090
M, N	183.027	194.742	22.048	-	-	0.620	0.234
M, K	199.758	74.403	41.956	-	-	0.626	0.228
N, K	209.810	-14.143	69.229	-	-	0.629	0.226
E, M, N	218.459	-0.310	76.680	24.884	-	0.795	0.291
E, M, K	237.437	-0.315	-59.385	47.775	-	0.807	0.275
E, N, K	226.872	-0.305	7.461	35.742	-	0.803	0.280
M, N, K	254.369	-304.961	-66.836	166.424	-	0.635	0.494
E, M, N, K	330.105	-0.330	-696.907	-111.174	255.097	0.829	0.584

* E: The empirical solvent polarity; M: Account for the solute permanent dipole-solvent-induced dipole; N: Solute permanent dipole-solvent permanent dipole interaction; K: Kirkwood's dielectric function; a_0: The regression intercept; a1, a2, a3, a4: coefficients; MCC: The multiple correlation coefficients and P: The probability of variation.

$$J = \frac{D-1}{D+2} \tag{4}$$

$$K = \frac{D-1}{2D+1} \tag{5}$$

$$N = J - H \tag{6}$$

$$H = \frac{n^2-1}{n^2+2} \tag{7}$$

E is the empirical solvent polarity that is sensitive to both solvent-solute hydrogen bonding and dipolar interactions related to ν_{max}, which is the wave number (cm^{-1}) of the absorption maximum of the given solvent. The Kirkwood dielectric function (K) represents the dipolar dielectric interactions and is a measure of the polarity of the solvent that depends on the dielectric constant (*D*) of the solvent.

The functions J and H have been introduced to account for nonspecific solute-solvent interactions such as dispersion and dipolar effects, respectively [30]. These are related to the dielectric constant (D) and the refractive index (n) of the solvent. The functions M and N have been introduced to account for the solute permanent dipole-solvent induced dipole and solute permanent dipole-solvent permanent dipole interactions, respectively [31]. The values of the solvent parameters K, M, N, E, D, and n in different solvents [32] are collected in Table 4.

The intercept a_0, and the coefficients a_1, a_2, ..., a_n have been calculated by multiple regression analysis using a micro-statistics SPSS program (Statistical package of social science program). In each case, fits are obtained as a function of one parameter alone, two parameters, three parameters, or four parameters. The results of the calculations for the compounds under investigation are collected in Tables 5 and 6.

Multiple correlation coefficients (R) or (MCC) and probability of variation (p) have been considered as a measure of goodness of fit. The high value of MCC (near one) means that a certain solvent parameter has a good correlation with the spectral shift. Therefore, the spectral shifts of the peak are greatly sensitive to the solvent parameter, which gives a value of MCC near unity. Alternatively, the small value (near zero) of the significance parameter (P) assigned a good correlation [33].

For the equation of one parameter of morpholine, the MCC and P values, the E parameter plays an important role in determining the spectral shifts that occurred for MOR at wavelength region y_1. This is provided by the high value of MCC (0.9) (near one) and the low value of P = 0.001, so the spectral shift in this region is affected by the polarity and ability of the formation of H bonds of the solvents.

Table 6. Regression analysis data for morpholine complexes.

Parameters	**$[Fe(MOR)_3Cl_3]\cdot 4H_2O$**				**$[Ni(MOR)_4Cl_2]\cdot 4H_2O$**			
	***y* = 234-256 nm**		***y* = 274-282 nm**		***y* = 223-244 nm**		***y* = 260-280 nm**	
	MCC	**P**	**MCC**	**P**	**MCC**	**P**	**MCC**	**P**
E	0.836	0.004	0.840	0.004	0.646	0.029	0.761	0.010
M	0.926	0.001	0.844	0.003	0.712	0.017	0.828	0.004
N	0.843	0.004	0.716	0.016	0.875	0.002	0.750	0.012
K	0.765	0.010	0.636	0.032	0.924	0.001	0.706	0.018
E, M	0.947	0.003	0.897	0.011	0.729	0.073	0.851	0.022
E, N	0.901	0.010	0.851	0.022	0.876	0.015	0.810	0.036
E, K	0.876	0.015	0.843	0.025	0.924	0.006	0.801	0.039
M, N	0.926	0.005	0.857	0.021	0.906	0.009	0.828	0.030
M, K	0.926	0.005	0.854	0.021	0.931	0.005	0.829	0.029
N, K	0.913	0.008	0.807	0.037	0.940	0.004	0.769	0.053
E, M, N	0.948	0.020	0.921	0.037	0.909	0.046	0.853	0.091
E, M, K	0.948	0.020	0.918	0.039	0.933	0.029	0.851	0.093
E, N, K	0.941	0.024	0.892	0.058	0.945	0.022	0.815	0.128
M, N, K	0.926	0.033	0.861	0.084	0.953	0.017	0.887	0.062
E, M, N, K	0.949	0.100	0.925	0.144	0.955	0.087	0.911	0.171
Parameters	**$[Cu(MOR)_4Cl_2]\cdot 6H_2O$**				**$[CuNi(MOR)_2Cl_4]\cdot 4H_2O$**			
	***y* = 217-230 nm**		***y* = 223-250 nm**		***y* = 230-236 nm**		***y* = 293-310 nm**	
	MCC	**P**	**MCC**	**P**	**MCC**	**P**	**MCC**	**P**
E	0.776	0.020	0.906	0.001	0.948	.000	0.665	0.025
M	0.975	0.001	0.875	0.002	0.748	0.012	0.696	0.020
N	0.915	0.003	0.806	0.006	0.692	0.020	0.854	0.003
K	0.829	0.012	0.730	0.014	0.630	0.033	0.907	0.001
E, M	0.975	0.004	0.950	0.003	0.948	0.003	0.726	0.075
E, N	0.919	0.023	0.928	0.005	0.948	0.003	0.855	0.021
E, K	0.859	0.053	0.917	0.007	0.949	0.003	0.908	0.008
M, N	0.978	0.003	0.876	0.015	0.748	0.063	0.882	0.014
M, K	0.976	0.004	0.875	0.016	0.748	0.063	0.914	0.007
N, K	0.992	0.001	0.875	0.016	0.743	0.066	0.928	0.005
E, M, N	0.978	0.032	0.951	0.018	0.953	0.017	0.891	0.059
E, M, K	0.977	0.035	0.952	0.018	0.953	0.017	0.922	0.036
E, N, K	0.993	0.010	0.955	0.016	0.954	0.016	0.943	0.023
M, N, K	0.992	0.012	0.879	0.068	0.749	0.196	0.956	0.016
E, M, N, K	0.993	0.122	0.956	0.087	0.954	0.090	0.964	0.070
Parameters	**$[CuZn(MOR)_3Cl_4]\cdot 2H_2O$**							
	***y* = 224-256 nm**		***y* = 253.5-265 nm**					
	MCC	**P**	**MCC**	**P**				
E	0.522	0.067	0.462	0.137				
M	0.308	0.196	0.615	0.065				
N	0.183	0.339	0.357	0.211				
K	0.121	0.445	0.263	0.298				
E, M	0.550	0.202	0.616	0.238				
E, N	0.677	0.104	0.462	0.394				
E, K	0.742	0.067	0.492	0.363				
M, N	0.432	.323	0.835	0.067				
M, K	0.458	0.294	0.822	0.075				
N, K	0.498	0.252	0.700	0.164				
E, M, N	0.751	0.194	0.849	0.217				
E, M, K	0.784	0.158	0.842	0.227				
E, N, K	0.812	0.131	0.772	0.321				
M, N, K	0.498	0.502	0.840	0.231				
E, M, N, K	0.822	0.324	0.850	0.553				

* E: The empirical solvent polarity; M: Account for the solute permanent dipole-solvent induced dipole; N: Solute permanent dipole-solvent permanent dipole interaction; K: Kirkwood's dielectric function; MCC: Multiple correlation coefficients, and P: The probability of variation.

For the wavelength region *y2,* the K parameter has a 0.61 value of MCC and a lower value of P = 0.067, indicating that the spectral shifts in this region are affected by the dielectric constant of the solvent. Based on the two parameters equation, the combination of E and M gave higher values of the correlation at wavelength region y_1 due to the high value of multiple regression (R) of 0.953 and the lower value of the probability of variation P = 0.002. Therefore, the solvent-solute hydrogen bonding ability combined with the solute permanent dipole-solvent-induced dipoles are the major factors causing the spectral shifts in these cases. The combination of E and K gave higher correlation values for morpholine in the wavelength region *y2,* as evident by its multiple regression coefficient (R) 0.799 and the low value of the probability of variation P = 0.09. It is concluded that the studied properties of the solvent are effective parameters to explain the spectral shifts for the compounds [34].

The data based on the three-parameter regression equation pointed to the relatively high value of multiple regression (MCC) and the lower value of the probability of variation (P) based on a combination of E, M, K parameters for both wavelength regions y_1 and y_2 occurred.

For the studied complexes based on one-parameter equation, the (M) gave a higher value of correlation for $[Fe(MOR)_3Cl_3]\cdot 4H_2O$ at both wavelength regions y_1 and y_2 with a value of 0.926 and 0.844 and a low P value of 0.001 and 0.003, respectively. For $[Ni(MOR)_4Cl_2]\cdot 4H_2O$ at wavelength region y_2 (MCC = 0.828, P = 0.004), $[Cu(MOR)_4Cl_2]\cdot 6H_2O$ at wavelength region y_1 (MCC = 0.975, P = 0.001), and $[CuZn(MOR)_3Cl_4]\cdot 2H_2O$ at wavelength region y_2 (MCC = 0.615, P = 0.065) indicating that solvatochromism can be interpreted in terms of permanent dipole-solvent-induced dipole interactions.

Parameter (E) gave a higher value of correlation for $[Cu(MOR)_4Cl_2]\cdot 6H_2O$ at wavelength region y_2 (MCC = 0.906, P = 0.001), also for $[CuNi(MOR)_2Cl_4]\cdot 4H_2O$ at wavelength region y_1 (MCC = 0.948, P = 0.001), and $[CuZn(MOR)_3Cl_4]\cdot 2H_2O$ at wavelength region y_1 (MCC = 0.522, P = 0.067), referred to that the solvent-solute hydrogen bonding and dipolar interactions are the major factors affecting the solvatochromism [35].

Table 7. K_1, K_2, ν_{vapour} and correlation analysis data for selected compounds.

Compound	**ν_{vapour} (cm^{1})**	**K_1**	**R(ν, D)**	**K_2**	**R(ν, n)**	**MCC**
Morpholine	45610.29	-2851.72	0.793	14760.93	0.684	0.656
$[Fe(MOR)_3Cl_3]\cdot 4H_2O$	34607.24	1628.65	0.794	-10344.60	0.917	0.856
$[Ni(MOR)_4Cl_2]\cdot 4H_2O$	33727.59	4178.39	0.827	-25165.83	0.906	0.821
$[Cu(MOR)_4Cl_2]\cdot 6H_2O$	36432.03	6893.39	0.836	-41691.92	0.919	0.845
$[CuNi(MOR)_2Cl_4]\cdot 4H_2O$	35335.69	-3059.20	0.947	14809.44	0.834	0.906
$[CuZn(MOR)_3Cl_4]\cdot 2H_2O$	41007.41	-2436.09	0.517	20868.55	0.782	0.839

* ν_{vapour}: The frequency of the peak maximum in the absence of solvents; K_1 and K_2: Proportional to the strength of the induction-dispersive and orientation interactions; R(ν, D), R(ν, n) and MCC: Multiple correlation coefficients.

The parameter (K) plays an important role in determining the spectral shifts for $[Ni(MOR)_4Cl_2]\cdot 4H_2O$ at wavelength region y_1 (MCC= 0.924, P = 0.001) and $[CuNi(MOR)_2Cl_4]\cdot 4H_2O$ at wavelength region y_2 (MCC =0.907, P = 0.001) this points to the fact that the dielectric constant is effective in explaining the spectral shifts. Based on the two-parameter equation, the combination of E and M gave higher correlation values for $[Fe(MOR)_3Cl_3]\cdot 4H_2O$ at both wavelength regions y_1 and y_2 (MCC =0.947,0.879, P = 0.003,0.011), $[Ni(MOR)_4Cl_2]\cdot 4H_2O$ at wavelength region y_2 (MCC = 0.851, P = 0.022) and $[Cu(MOR)_4Cl_2]\cdot 6H_2O$ at wavelength region y_2 (MCC = 0.950, P = 0.003), used to explain the spectral shifts occurred in these cases related to the solvent ability to form hydrogen bonds with the solute molecules, which is expressed by the parameter E combined with solute permanent dipole-solvent induced dipole interactions [36].

The solute permanent dipole-solvent permanent dipole interactions (N) combined with the dielectric constant (K) is used to explain the correlation by its high MCC values and low P values in the case of $[Cu(MOR)_4Cl_2]\cdot 6H_2O$ at wavelength region y_1 (MCC = 0.992, P = 0.001), $[CuNi(MOR)_2Cl_4]\cdot 4H_2O$ at wavelength region y_2 (MCC =0.928, P = 0.005) and $[Ni(MOR)_4Cl_2]\cdot 4H_2O$ at wavelength region y_1 (MCC = 0.940, P = 0.004). The combination of E and K parameters used to explain the spectral shift in case of $[CuNi(MOR)_2Cl_4].4H_2O$ at wavelength region y_1 (MCC =0.949, P = 0.003) and $[CuZn(MOR)_3Cl_4].2H_2O$ at wavelength region y_1 (MCC = 0.742, P =0.067) explained by that the ability of H-bond formation combined with the polarity of the solvent that depends on the dielectric constant has the major effect in this correlation [37]. The best correlation coefficient is observed with the combination of M and N functions for $[CuZn(MOR)_3Cl_4]\cdot 2H_2O$ at the wavelength region y_2 (MCC = 0.835, P =0.067). Thus, solvent spectral shifts are best affected by the solute permanent dipole-solvent induced dipole combinated with the solute permanent dipole-solvent permanent dipole interactions [38]. Based on the three parameters equation, the combination of (E, M, N) and (E, M, K) both showed high multiple regression (R) for $[Fe(MOR)_3Cl_3]\cdot 4H_2O$ at both wavelength regions y_1 (MCC = 0.948, P = 0.02) and $[CuNi(MOR)_2Cl_4]\cdot 4H_2O$ at wavelength region y_1 (MCC =0.953, P = 0.017) indicating the effect of E, M combined with N and K solvent parameters on the spectral shifts of these compounds. The combination of E, M, N that affects the correlation in case of $[Fe(MOR)_3Cl_3]\cdot 4H_2O$ at both wavelength regions y_2 (MCC =0.921, P = 0.037) and $[CuZn(MOR)_3Cl_4]\cdot 2H_2O$ at wavelength region y_2 (MCC =0.849, P = 0.217) indicating the effect of solvent hydrogen bond formation ability E, the permanent dipole-solvent induced dipole M and solute permanent dipole solvent permanent dipole interactions. M, N, and K parameters combination was effected in case of $[Ni\ (MOR)_4Cl_2]\cdot 4H_2O$ at both wavelength regions y_1 and y_2 (MCC = 0.953, 0.887, P = 0.017, 0.062) and for $[CuNi(MOR)_2Cl_4]\cdot 4H_2O$ at wavelength region y_2 (MCC = 0.956, P = 0.016). The combination of E, N, and K parameters shows the major effect in case of $[Cu(MOR)_4Cl_2]\cdot 6H_2O$ at both wavelength regions y_1 and y_2 (MCC = 0.993, 0.955, P = 0.01, 0.016) and $[CuZn(MOR)_3Cl_4]\cdot 2H_2O$ at wavelength region y_1 (MCC = 0.812, P = 0.131).

The following equation is applied [39]:

$$\nu_{Solution} = \nu_{Vapour} + K_1\left(\frac{2D-2}{2D+1}\right) + K_2\left(\frac{2n^2-2}{2n^2+1}\right) \tag{8}$$

where $x_2 = \dfrac{2n^2-2}{2n^2+1}$, $x_1 = \dfrac{2D-2}{2D+1}$ and $\nu_{Solution}$ is the frequency of the peak maximum in the presence of solvents; D, dielectric constant; n, refractive index and ν_{Vapour} is the frequency of the peak maximum in the absence of solvents. The K_1 and K_2 are proportional to the strength of induction-dispersive and orientation interactions, respectively. Multiple regression techniques were used to evaluate ν_{Vapour} values, the coefficients K_1 and K_2, R (ν, D), R (ν, n), and MCC (Table 7). The data indicated that both the dielectric constant (D) and the refractive index (n) of the solvents affect the electronic absorption spectra of these compounds, but to different degrees. For simplicity, ν_{Vapour} values were calculated when K_2 = zero and the equation becomes as follows:

$$\nu_{Solution} = \nu_{Vapour} + K_1\left(\frac{2D-2}{2D+1}\right) \tag{9}$$

where $\nu_{(solution)}$ values were plotted against x_1 and the values of K_1 and ν_{vapour} were obtained from the slopes and the intercepts, respectively (Figure 4). Multiple correlation coefficients R(ν, D) were calculated using an SPSS program (Table 7). Similarly, ν_{vapour} were calculated when K_1 = zero and the equation becomes as follows:

$$\nu_{Solution} = \nu_{Vapour} + K_2\left(\frac{2n^2-2}{2n^2+1}\right) \tag{10}$$

where $\nu_{Solution}$ values were plotted against x_2 and the values of K_2 and ν_{Vapour} were obtained from the slopes and intercepts, respectively, (Figure 5), and the multiple correlation coefficients R(ν, n) were calculated using the SPSS program (Table 7).

The calculated K_1, K_2, ν_{Vapour}, R(ν, D), R(ν, n) and MCC for all investigated compounds point that both the dielectric constant and the refractive index of solvents affect the electronic spectral properties of the compounds with different degrees. The high values (near one) of R(ν, D) in case of morpholine and $[CuNi(MOR)_2Cl_4]\cdot 4H_2O$ complex only the dielectric constant (D) function had the stronger effect than that of refractive index (n), so the peak shifts should depend primarily upon dielectric constant (D). On the other hand, for $[Fe(MOR)_3Cl_3]\cdot 4H_2O$, $[Ni(MOR)_4Cl_2]\cdot 4H_2O$, $[Cu(MOR)_4Cl_2]\cdot 6H_2O$ and $[CuZn(MOR)_3Cl_4]\cdot 2H_2O$ R(ν, n) has a high value (near one) meaning that the spectral shifts observed using different solvents with different parameters depend on the refractive index (n).

3.4. Radius of solutes calculations

Solvation describes the interaction of solvent with molecules or ions in a solute. Ions and, in some cases, molecules, interact strongly with the solvent, and the strength and nature of this interaction influence many properties of the solute, including solubility and reactivity [40]. Solvation is the process of reorganizing solvent and solute molecules into solvation complexes.

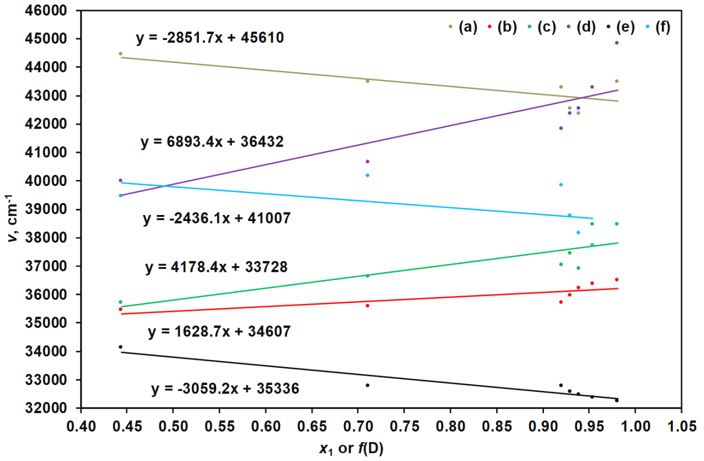

Figure 4. ν *vs* - x_1, *f*(D) plots of (a) morpholine, (b) $[Fe(MOR)_3Cl_3]\cdot 4H_2O$, (c) $[Ni(MOR)_4Cl_2]\cdot 4H_2O$, (d) $[Cu(MOR)_4Cl_2]\cdot 6H_2O$, (e) $[CuNi(MOR)_2Cl_4]\cdot 4H_2O$, and (f) $[CuZn(MOR)_3Cl_4]\cdot 2H_2O$.

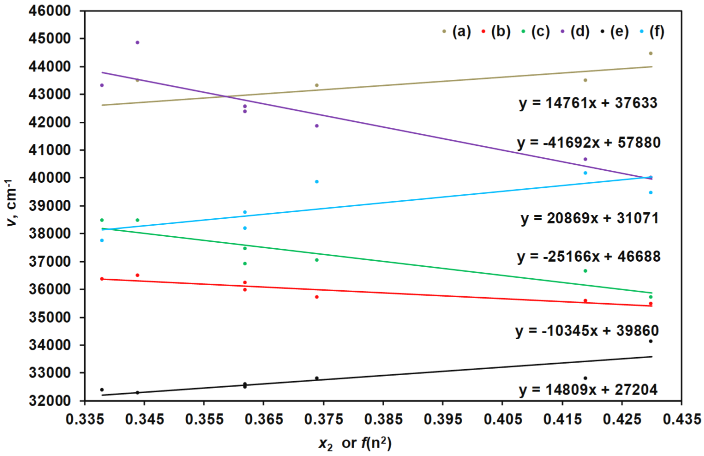

Figure 5. ν *vs* - x_2, *f*(n^2) plots of (a) morpholine, (b) $[Fe(MOR)_3Cl_3]\cdot 4H_2O$, (c) $[Ni(MOR)_4Cl_2]\cdot 4H_2O$, (d) $[Cu(MOR)_4Cl_2]\cdot 6H_2O$, (e) $[CuNi(MOR)_2Cl_4]\cdot 4H_2O$, and (f) $[CuZn(MOR)_3Cl_4]\cdot 2H_2O$.

Solvent-solute interactions play a key role in solution-phase chemistry. Solvent-solute interactions are thus often essential in the determination of ground states and steering chemical reactions in solution-phase chemistry. Solvation involves bond formation, hydrogen bonding, and Vander Waals forces [41]. The energy of solvation is the amount of energy associated with the dissolution of a solute in a solvent. The reaction field model of solute-solvent interactions introduced by the Onsager Equation (11) [42] is the most widely used for the solvent-solute interaction.

$$E^{dipol}_{Solv} = \frac{-\mu^2}{2a^3} f(D) \qquad (11)$$

$$f(D) = \frac{2D\text{-}2}{2D+1} \qquad (12)$$

The solvent polarity function [43] *f*(D) is a dimensionless number; that represents the relative strength of the electric field experienced by the ion or dipole, respectively. A neutral dipolar molecule is a sphere with a central point dipole moment μ.

The ν values were plotted versus *f*(D) for the compounds under investigation; Radii (a) were calculated from the slope = $\frac{-\mu^2}{2a^3}$, (Figure 4, Table 8). The E^{dipol}_{Solv} values based on dipole polarization, Equation (11), were calculated, and data were collected in Table 8. Morpholine and its mixed metal complexes $[CuNi(MOR)_2Cl_4]\cdot 4H_2O$ and $[CuZn(MOR)_3Cl_4]\cdot 2H_2O$ show negative slopes, leading to positive values and E^{dipol}_{Solv} values were negative to support that the main solvent-solute interac-tion is a dipole-dipole interaction.

The dipole produces an electric field. This field has two separate effects on the surrounding solvent molecules.

i) Induction polarization, where the solute-solvent interaction is given by

$$E_{Solv} = \frac{-\mu_M}{a_M^3} f(n^2) \qquad (13)$$

where $f(n^2) = \frac{2(n^2-1)}{2n^2+1}$. Equation (13), is a measure of permanent dipole-induced dipole interactions between the solute and the solvent, while a_M is the radius of the spherical cavity which contains the solvent molecule. The ν values were plotted versus *f*(n^2) and the radii a_M were calculated from the slope = $-\mu_M/a_M^3$ (Figure 5 and Table 8). Morpholine and its mixed metal complexes $[CuNi(MOR)_2Cl_4]\cdot 4H_2O$ and $[CuZn(MOR)_3Cl_4]\cdot 2H_2O$ had a positive slope that leads to the fact that the a_M values are negative indicating the heterogeneous distribution of solvent surrounding the solute except in the case of $[Fe(MOR)_3Cl_3]\cdot 4H_2O$, $[Ni(MOR)_4Cl_2]\cdot 4H_2O$ and $[Cu(MOR)_4Cl_2]\cdot 6H_2O$ are positive that they have a negative slope and positive a_M values refer to a homogeneous distribution of solvent surrounding the solute.

Table 8. Values of a and E_{Solv}^{dipol} based on dipole polarization introduced by the Onsager equation.

Compound/solvent		CCl$_4$	CHCl$_3$	*i*-Propanol	Acetone	Ethanol	Methanol	Water
Morpholine	a	-	0.0575	0.0785	0.1133	0.0794	-	0.0843
	E_{Solv}^{dipol}	-1266.15	-2027.56	-2623.56	-2652.08	-2677.75	-	-2797.52
[Fe(MOR)$_3$Cl$_3$]·4H$_2$O	a	-	-0.0692	-0.0946	-0.1365	-0.0957	-0.0961	-0.1017
	E_{Solv}^{dipol}	723.14	1158.01	1498.40	1514.69	1529.35	1553.78	1597.75
[Ni(MOR)$_4$Cl$_2$]·4H$_2$O	a	-	-0.0506	-0.0691	-0.0997	-0.0699	-0.0702	-0.0743
	E_{Solv}^{dipol}	1855.21	2970.84	3844.13	3885.91	3923.52	3986.19	4099.01
[Cu(MOR)$_4$Cl$_2$]·6H$_2$O	a	-	-0.0428	-0.0585	-0.0844	-0.0592	-0.0594	-0.0628
	E_{Solv}^{dipol}	3060.67	4901.21	6341.93	6410.86	6472.90	6576.30	6762.43
[CuNi(MOR)$_2$Cl$_4$]·4H$_2$O	a	-	0.0561	0.0767	0.1107	0.0776	0.0779	0.0824
	E_{Solv}^{dipol}	-1358.28	-2175.09	-2814.41	-2845.06	-2872.59	-2918.48	-3001.08
[CuZn(MOR)$_3$Cl$_4$]·2H$_2$O	a	-	0.0605	0.0827	0.1194	0.0837	0.0840	-
	E_{Solv}^{dipol}	-1081.63	-1732.07	-2241.21	-2265.57	-2287.49	-2324.04	-

Table 9. Values of a_M and E_{solv} based on induction polarization obtained by applying Equation (5).

Compound/solvent		CCl$_4$	CHCl$_3$	*i*-Propanol	Acetone	Ethanol	Methanol	Water
Morpholine	a_M	-	-0.0413	-0.0483	-0.0579	-0.0486	-	-0.0500
	E_{solv}	6347.23	6184.86	5520.61	5343.48	5343.48	-	5077.78
[Fe(MOR)$_3$Cl$_3$]·4H$_2$O	a_M	-	0.0465	0.0543	0.0653	0.0547	0.0548	0.0563
	E_{solv}	-4448.35	-4334.56	-3869.03	-3744.89	-3744.89	-3496.61	-3558.68
[Ni(MOR)$_4$Cl$_2$]·4H$_2$O	a_M	-	0.0346	0.0404	0.0486	0.0406	0.0407	0.0419
	E_{solv}	-10821.38	-10544.55	-9412.08	-9110.09	-9110.09	-8506.11	-8657.10
[Cu(MOR)$_4$Cl$_2$]·6H$_2$O	a_M	-	0.0292	0.0341	0.0410	0.0343	0.0344	0.0354
	E_{solv}	-17927.56	-17468.95	-15592.81	-15092.50	-15092.50	-14091.89	-14342.05
[CuNi(MOR)$_2$Cl$_4$]·4H$_2$O	a_M	-	-0.0413	-0.0482	-0.0579	-0.0485	-0.0486	-0.0499
	E_{solv}	6367.87	6204.97	5538.57	5360.86	5360.86	5005.44	5094.29
[CuZn(MOR)$_3$Cl$_4$]·2H$_2$O	a_M	-	-0.0367	-0.0430	-0.0517	-0.0432	-0.0433	-
	E_{solv}	8973.67	8744.11	7805.01	7554.58	7554.58	7053.72	-

The E_{solv} values based on induction polarization were calculated for the compounds investigated from Equation (13) and the data are collected (Table 9). The positive values of E_{solv} in the case of morpholine and its mixed metal complexes [CuNi(MOR)$_2$Cl$_4$]·4H$_2$O and [CuZn(MOR)$_3$Cl$_4$]·2H$_2$O assigned to the transitions from the ground to the excited states while the negative values of E_{solv} in the case of [Fe(MOR)$_3$Cl$_3$]·4H$_2$O, [Ni(MOR)$_4$Cl$_2$]·4H$_2$O and [Cu(MOR)$_4$Cl$_2$]·6H$_2$O assigned to the transitions from the excited to ground states.

ii) Orientation polarization, where the solute-solvent interaction is given by

$$E_{Solv} = \frac{-\mu_M}{2a_M^3}\left[f(D) - f(n^2)\right] \qquad (14)$$

whereas, f(D, n^2), is a measure of interactions between the permanent dipole [44]. However, the υ values were plotted versus $\left[f(D) - f(n^2)\right]$ relation and the radii of solvation a_M were calculated from the slope = $\frac{-\mu_M}{2a_M^3}$ (Figure 6, Table 10). The E_{solv} values based on orientation polarization, Equation (14), were calculated and the data are collected in Table 10. The nature, type, intensity, and position of the absorption bands may be significantly affected by the type of solvent.

3.5. Solvent interactions

Kamlet and Taft method is the most widely applied method for generating values for intermolecular solute/solvent interactions [45,46]. The overall solvent effect has been successfully applied to separate the influence of specific and nonspecific chemical interactions. The nonspecific chemical interactions including electrostatic effects (dipolarity/ polarizability) and the specific interactions including hydrogen bonding are related to the molecular structure of the compound [47,48]. The effects of solvent polarity and hydrogen bonding on the absorption spectra were interpreted by the linear solvation energy relationships (LSER) concept using a general Equation (15):

$$\nu_{max} = \nu_{\circ} + s\pi^* + a\alpha + b\beta \qquad (15)$$

where, ν_{max} is the wavenumber (cm^{-1}) of the maximum absorption band in pure solvents (Table 11), ν_o is the regression intercept corresponds to the gaseous of the spectrally active compounds, (s, a and b) are the solvatochromic coefficients while (π^*, α and β) are the solvatochromic parameters.

In these equations, π^* is an index of the dipolarity / polarizability of the solvent which is a measure of the ability of the solvent to stabilize a charge or a dipole by its own dielectric effects [49]. The π^* scale was selected to run from 0.00 for cyclohexanone to 1.00 for dimethylsulfoxide. The variable α is a measure of the solvent hydrogen bond donor (HBD) acidity, and describes the ability of the solvent to donate a proton in a solvent-to-solute hydrogen bond. The scale α was selected to extend from 0.00 for non-HBD solvents to approximately 1.00 for methanol. The variable β is a measure of the solvent hydrogen- bond acceptor (HBA) basicity [50] and describes the ability of the solvent to accept a proton in a solute-to-solvent hydrogen bond. The scale β was selected to extend from 0.00 for non-HBD solvents to approximately 1.00 for hexamethyl phosphoric acid triamide. ν_o, a, b, and s are solvent-independent constants, their magnitudes and sign provide measures of the influence of the corresponding solute-solvent interactions on the wavenumber in the maximum of the electronic absorption band, which have been determined by multiple regression analysis using the SPSS statistical program. The solvent parameters [51,52] are given in Table 12.

The results of the correlation of the absorption frequencies with the solvatochromic parameters (π^*, α, and β) are given in Table 13. The percentage contribution of the calculated solvatochromic parameters from the values of the regression coefficients is given in Table 14 (Figure 7).

Table 10. Values of a_M and E_{solv} based on orientation polarization obtained by applying Equation (6).

Compound/solvent		**CCl_4**	**$CHCl_3$**	**i-propanol**	**Acetone**	**Ethanol**	**Methanol**	**Water**
Morpholine	a_M	-	0.0598	0.0699	0.0839	0.0703	-	0.0724
	E_{solv}	-34.09	-710.99	-1329.46	-1383.02	-1404.94	-	-1551.03
$[Fe(MOR)_3Cl_3]\cdot 4H_2O$	a_M	-	-0.0712	-0.0832	-0.0999	-0.0837	-0.0839	-0.0863
	E_{solv}	20.17	420.77	786.79	818.49	831.46	887.66	917.92
$[Ni(MOR)_4Cl_2]\cdot 4H_2O$	a_M	-	-0.0522	-0.0609	-0.0733	-0.0613	-0.0614	-0.0632
	E_{solv}	51.29	1069.83	2000.43	2081.04	2114.01	2256.90	2333.84
$[Cu(MOR)_4Cl_2]\cdot 6H_2O$	a_M	-	-0.0441	-0.0516	-0.0619	-0.0518	-0.0519	-0.0535
	E_{solv}	84.68	1766.19	3302.54	3435.60	3490.04	3725.94	3852.96
$[CuNi(MOR)_2Cl_4]\cdot 4H_2O$	a_M	-	0.0585	0.0684	0.0822	0.0688	0.0689	0.0709
	E_{solv}	-36.33	-757.74	-1416.87	-1473.96	-1497.32	-1598.52	-1653.02
$[CuZn(MOR)_3Cl_4]\cdot 2H_2O$	a_M	-	0.0611	0.0714	0.0858	0.0718	0.0719	-
	E_{solv}	-31.94	-666.08	-1245.48	-1295.66	-1316.19	-1405.16	-

Table 11. ν_{max} of electronic absorption spectra (cm^{-1}) in different solvents for morpholine and its complexes in the presence of different solvents.

Compound	**CCl_4**	**$CHCl_3$**	***i*-Propanol**	**Acetone**	**Ethanol**	**Methanol**	**Water**
Morpholine	44444.44	43478.26	43290.04	42553.19	42372.88	-	43478.26
$[Fe(MOR)_3Cl_3]\cdot 4H_2O$	35460.99	35587.18	35714.28	35971.22	36231.88	36363.63	36496.35
$[Ni(MOR)_4Cl_2]\cdot 4H_2O$	35714.28	36630.03	37037.03	37453.18	36900.36	38461.53	38461.53
$[Cu(MOR)_4Cl_2]\cdot 6H_2O$	40000	40650.40	41841.00	42372.88	42553.19	43290.04	44843.04
$[CuNi(MOR)_2Cl_4]\cdot 4H_2O$	34129.69	32786.88	32786.88	32573.28	32467.53	32362.45	32258.06
$[CuZn(MOR)_3Cl_4]\cdot 2H_2O$	39447.73	40160.64	39840.63	38759.68	38167.93	37735.84	-

Table 12. Solvatochromic parameters.

Solvent	**π***	**α**	**β**
CCl_4	0.28	0.00	0.00
$CHCl_3$	0.58	0.20	0.10
i-Propanol	0.48	0.76	0.95
Acetone	0.71	0.08	0.43
Ethanol	0.54	0.83	0.77
Methanol	0.60	0.93	0.62
Water	1.09	1.17	0.18

Table 13. Solvent independent correlation coefficient of π*, α and β solvatochromic parameters *.

Compound	**ν_o**	**s**	**a**	**b**	**MCC**
Morpholine	444906.810	-2206.276	-1007.012	-1961.320	0.842
$[Fe(MOR)_3Cl_3]\cdot 4H_2O$	35220.944	752.911	433.372	110.221	0.881
$[Ni(MOR)_4Cl_2]\cdot 4H_2O$	35038.309	2658.560	549.237	600.219	0.880
$[Cu(MOR)_4Cl_2]\cdot 6H_2O$	38527.271	4287.287	1325.837	736.554	0.962
$[CuNi(MOR)_2Cl_4]\cdot 4H_2O$	34459.138	-2106.167	74.056	-1025.836	0.915
$[CuZn(MOR)_3Cl_4]\cdot 2H_2O$	40495.219	-2060.802	-1851.028	1009.746	0.623

* ν_o: The regression intercept corresponds to the gaseous of the spectrally active compounds; s, a, b: The solvatochromic coefficients; MCC: Multiple correlation coefficients.

Table 14. Percentage of contribution of π*, α and β solvatochromic parameters #.

Compound	**P_{π^*} (%)**	**P_α (%)**	**P_β (%)**
Morpholine	42.64	19.46	37.90
$[Fe(MOR)_3Cl_3]\cdot 4H_2O$	58.07	33.43	8.50
$[Ni(MOR)_4Cl_2]\cdot 4H_2O$	69.81	14.42	15.77
$[Cu(MOR)_4Cl_2]\cdot 6H_2O$	67.52	20.88	11.60
$[CuNi(MOR)_2Cl_4]\cdot 4H_2O$	65.69	2.31	32.00
$[CuZn(MOR)_3Cl_4]\cdot 2H_2O$	41.87	37.61	20.52

P_{π^*}(%): The percentage contribution of the ability of the solvent to stabilize a charge or a dipole by its own dielectric effects, P_α(%): The percentage contribution of the solvent hydrogen-bond donor (HBD) acidity, P_β(%): The percentage contribution of the solvent hydrogen- bond acceptor (HBA) basicity.

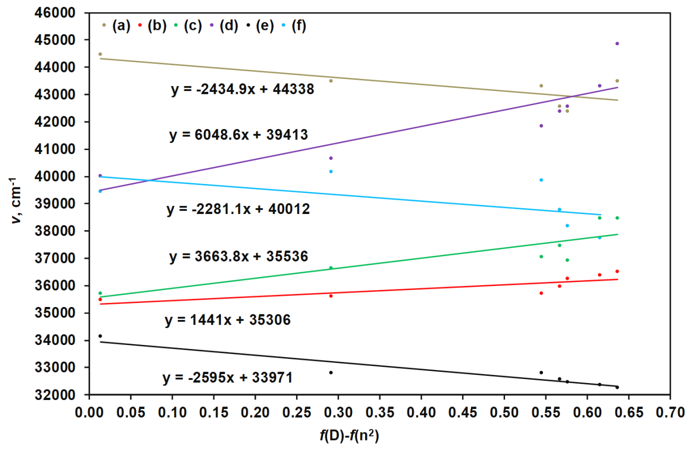

Figure 6. ν *vs* - $\left[f(D)-f(n^2)\right]$ plots of (a) Morpholine, (b) $[Fe(MOR)_3Cl_3]\cdot 4H_2O$, (c) $[Ni(MOR)_4Cl_2]\cdot 4H_2O$, (d) $[Cu(MOR)_4Cl_2]\cdot 6H_2O$, (e) $[CuNi(MOR)_2Cl_4]\cdot 4H_2O$, and (f) $[CuZn(MOR)_3Cl_4]\cdot 2H_2O$.

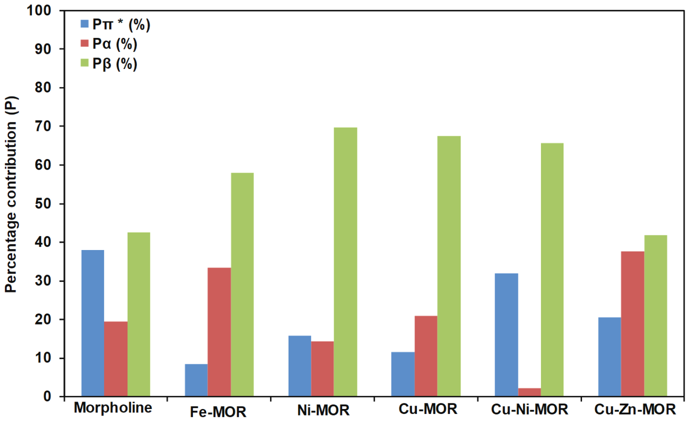

Figure 7. Percentage contribution (P) to the solvatochromic effects applying Equation (15).

The results show that the contributions to the solvatochromic shift arise from dipolarity/polarizability (π*) arising from the high values of coefficient (s) shown in Table 14. The highest negative value of the MCC coefficient in $[Cu(MOR)_4Cl_2]\cdot6H_2O$ indicates a better stabilization of the transition state by dipolarity / polarizability, due to the ability of the solvent to stabilize a charge or a dipole by its own dielectric effects. The percentage contributions of the calculated solvatochromic parameters show that the classic solvation effects play a major role in explaining the spectral shifts in all investigated complexes.

4. Conclusions

The optical absorption spectra of morpholine and its five morpholine complexes have been examined in various solvents of various polarities. Morpholine and both the $[CuNi(MOR)_2Cl_4]\cdot4H_2O$ and $[CuZn(MOR)_3Cl_4]\cdot2H_2O$ complexes reveal a red shift due to the solute-solvent interactions causing destabilization of the solute ground electronic state with increasing solvent polarity. $[Fe(MOR)_3Cl_3]\cdot4H_2O$, $[Ni(MOR)_4Cl_2]\cdot4H_2O$, and $[Cu(MOR)_4Cl_2]\cdot6H_2O$ complexes suffering a blue shift related to the formation of hydrogen bonds, suggesting the destabilization of the excited state compared to the electronic state of the ground. For morpholine, $[Fe(MOR)_3Cl_3]\cdot4H_2O$, $[Ni(MOR)_4Cl_2]\cdot4H_2O$ and $[Cu(MOR)_4Cl_2]\cdot6H_2O$ complexes the solvent-solute hydrogen bonding ability combined with the solute permanent dipole-solvent induced dipoles are the major factors that affecting their absorption spectra due to the high values of the correlation coefficient (near one) and lower values of the probability of variation. The solvent spectral shifts of $[CuNi(MOR)_2Cl_4]\cdot4H_2O$ and $[CuZn(MOR)_3Cl_4]\cdot2H_2O$ complexes are best affected by the solute permanent dipole-solvent permanent dipole combined with the solute permanent dipole-solvent induced dipole interactions. Solvation energy was defined quantitatively as the energy of interaction between the solute and the solvent. Born (point charge model) and Onsager (point dipole dielectric continuum model) formulations are two important and commonly used formulations for solvent-solute interactions.

Disclosure statement DS

Conflict of interest: There are no financial conflicts of interest to disclose.
Ethical approval: All ethical guidelines have been adhered to.
Sample availability: Samples of the compounds are available.

CRediT authorship contribution statement CR

Conceptualization: Mamdouh Saad Masoud, Alaa Eldin Ali; Methodology: Gehan Shabaan Elasala, Rehab Elsaid Elwardany; Software: Rehab Elsaid Elwardany Validation: Mamdouh Saad Masoud, Alaa Eldin Ali, Gehan Shabaan Elasala, Rehab Elsaid Elwardany; Formal Analysis: Alaa Eldin Ali, Rehab Elsaid Elwardany; Investigation: Rehab Elsaid Elwardany; Resources: Rehab Elsaid Elwardany; Data Curation: Rehab Elsaid Elwardany; Writing - Original Draft: Rehab Elsaid Elwardany; Writing - Review and Editing: Mamdouh Saad Masoud, Alaa Eldin Ali, Rehab Elsaid Elwardany; Funding acquisition: no funding; Supervision: Mamdouh Saad Masoud, Alaa Eldin Ali, Gehan Shabaan Elasala; Project Administration: Mamdouh Saad Masoud, Alaa Eldin Ali, Gehan Shabaan Elasala, Rehab Elsaid Elwardany.

ORCID iD and Email ✉

Mamdouh Saad Masoud
✉ drmsmasoud@yahoo.com
iD https://orcid.org/0000-0003-0320-6234
Alaa Eldin Ali
✉ dralaae@yahoo.com
iD https://orcid.org/0000-0003-0437-8919
Gehan Shaaban Elasala
✉ drgehanelasala@gmail.com
iD https://orcid.org/0000-0003-3032-5992
Rehab Elsaid Elwardany
✉ rehabelwardany@sci.dmu.edu.eg
✉ rehabelwardany4@gmail.com
iD https://orcid.org/0000-0001-9248-146X

References

[1]. Duhalde, V.; Lahille, B.; Camou, F.; Pédeboscq, S.; Pometan, J.-P. Bon usage des antibiotiques: étude prospective sur l'utilisation du linézolide dans un hôpital universitaire français. *Pathol. Biol. (Paris)* **2007**, *55*, 478–481.

[2]. Marcireau, C.; Guilloton, M.; Karst, F. In vivo effects of fenpropimorph on the yeast Saccharomyces cerevisiae and determination of the molecular basis of the antifungal property. *Antimicrob. Agents Chemother.* **1990**, *34*, 989–993.

[3]. de Almeida, K. J.; Ramalho, T. C.; Rinkevicius, Z.; Vahtras, O.; Agren, H.; Cesar, A. Theoretical study of specific solvent effects on the optical and magnetic properties of copper(II) acetylacetonate. *J. Phys. Chem. A* **2011**, *115*, 1331–1339.

[4]. Kosenkov, D.; Slipchenko, L. V. Solvent effects on the electronic transitions of p-nitroaniline: a QM/EFP study. *J. Phys. Chem. A* **2011**, *115*, 392–401.

[5]. Gülseven Sıdır, Y.; Sıdır, I.; Taşal, E.; Ermiş, E. Studies on the electronic absorption spectra of some monoazo derivatives. *Spectrochim. Acta A Mol. Biomol. Spectrosc.* **2011**, *78*, 640–647.

[6]. Adegoke, O. A.; Idowu, O. S. Solvatochromic behaviours and structure-spectra relationships of 4-carboxyl-2,6-dinitrophenylazohydroxy naphthalenes. *Spectrochim. Acta A Mol. Biomol. Spectrosc.* **2010**, *75*, 719–727.

[7]. Baughman, B. M.; Stennett, E.; Lipner, R. E.; Rudawsky, A. C.; Schmidtke, S. J. Structural and spectroscopic studies of the photophysical properties of benzophenone derivatives. *J. Phys. Chem. A* **2009**, *113*, 8011–8019.

[8]. Reichardt, C. Solvatochromic dyes as solvent polarity indicators. *Chem. Rev.* **1994**, *94*, 2319–2358.

[9]. Warde, U.; Sekar, N. Solvatochromic benzo[h] coumarins: Synthesis, solvatochromism, NLO and DFT study. *Opt. Mater. (Amst.)* **2017**, *72*, 346–358.

[10]. Masoud, M. S.; Shaker, M. A.; Ali, A. E.; Elasal, G. S. Solvatochromaticity and pH dependence of the electronic absorption spectra of some purines and pyrimidines and their metal complexes. *Spectrochim. Acta A Mol. Biomol. Spectrosc.* **2011**, *79*, 538–547.

[11]. Van Uitert, L. G.; Haas, C. G. Studies on coördination compounds. I. a method for determining thermodynamic equilibrium constants in mixed Solvents1, 2. *J. Am. Chem. Soc.* **1953**, *75*, 451–455.

[12]. Masoud, M. S.; Ali, A. E.; Elasala, G. S.; Elwardany, R. E. Structural and thermal studies on some morpholine complexes. *J. Mol. Struct.* **2019**, *1175*, 648–662.

[13]. Knapp, J. S.; Emtiazl, G.; Yusoff, S.; Heron, S. T. The utilization of morpholine as a sole nitrogen source by Gram-negative bacteria. *Letters in Applied Microbiology* **1996**, *23*, 334–338.

[14]. Knapp, J. S.; Whytell, A. J. The biodegradation of morpholine in river water and activated sludge. *Environ. Pollut.* **1990**, *68*, 67–79.

[15]. Díaz, M. S.; Freile, M. L.; Gutiérrez, M. I. Solvent effect on the UV/Vis absorption and fluorescence spectroscopic properties of berberine. *Photochem. Photobiol. Sci.* **2009**, *8*, 970–974.

[16]. Hanesch; Scholger Mapping of heavy metal loadings in soils by means of magnetic susceptibility measurements. *Environ. Geol.* **2002**, *42*, 857–870.

[17]. Ahuja, I. S.; Singh, R. Morpholine complexes with divalent nickel thiocyanate. *Transit. Met. Chem.* **1977**, *2*, 132–135.

[18]. Ahuja, I. S.; Singh, R. Bidentate bridged morpholine complexes with zinc(II) and cadmium(II) cyanides. *J. Coord. Chem.* **1976**, *5*, 167–170.

[19]. Kramer, P.; Nowak, T. The preparation and characterization of Cr(III) and Co(III) complexes of GDP and GTP and their interactions with avian phosphoenolpyruvate carboxykinase. *J. Inorg. Biochem.* **1988**, *32*, 135–151.

[20]. Jogi, P.; Mounika, K.; Padmaja, M.; M., L.; Gyanakumari, C. Synthesis, characterization and antibacterial studies of some transition metal complexes of a Schiff base derived from 2-(aminomethyl)-benzimidazole and thiophene-2-carbaxaldehyde. *E-J. Chem.* **2011**, *8*, 1662–1669.

[21]. Tabbì, G.; Giuffrida, A.; Bonomo, R. P. Determination of formal redox potentials in aqueous solution of copper(II) complexes with ligands having nitrogen and oxygen donor atoms and comparison with their EPR and UV-Vis spectral features. *J. Inorg. Biochem.* **2013**, *128*, 137–145.

[22]. Figgins, P. E.; Busch, D. H. Complexes of Iron(II), Cobalt(II) and Nickel(II) with Biacetyl-bis-methylimine, 2-Pyridinal-methylimine and 2,6-Pyridindial-bis-methylimine. *J. Am. Chem. Soc.* **1960**, *82*, 820–824.

[23]. Anan, N. A.; Hassan, S. M.; Saad, E. M.; Butler, I. S.; Mostafa, S. I. Preparation, characterization and pH-metric measurements of 4-hydroxysalicylidenechitosan Schiff-base complexes of Fe(III), Co(II), Ni(II), Cu(II), Zn(II), Ru(III), Rh(III), Pd(II) and Au(III). *Carbohydr. Res.* **2011**, *346*, 775–793.

[24]. Louis, C.; Che, M. EPR investigation of the coordination sphere of molybdenum(5+) ions on thermally reduced silica-supported molybdenum catalysts prepared by the grafting method. *J. Phys. Chem.* **1987**, *91*, 2875–2883.

[25]. Husain, M. M.; Sindhu, R.; Tandon, H. C. Determination of excited singlet-state dipole moments of hydroxy and methoxy coumarins using solvatochromic method. *Eur. J. Chem.* **2012**, *3*, 75–80.

[26]. George, J.; George, M.; Alex, J.; Sajan, D.; Shihab, N. K.; Vinitha, G.; Chitra, R. Growth of Morpholin-4-ium hydrogen tartrate single crystal for optical limiting application. *Opt. Laser Technol.* **2019**, *119*, 105647.

[27]. Airinei, A.; Homocianu, M.; Dorohoi, D. O. Changes induced by solvent polarity in electronic absorption spectra of some azo disperse dyes. *J. Mol. Liq.* **2010**, *157*, 13–17.

[28]. Iwanek, W.; Mattay, J. Ground state and excited state association: chiral recognition between 2,2′-dihydroxy-1,1′-binaphthyl and amines. *J. Photochem. Photobiol. A Chem.* **1992**, *67*, 209–226.

[29]. David, J. G.; Hallam, H. E. Infra-red solvent shifts and molecular interactions—X triatomic molecules, CS2, COS and SO2. *Spectrochim. Acta A* **1967**, *23*, 593–603.

[30]. Abe, T. Theory of solvent effects on molecular electronic spectra. Frequency shifts. *Bull. Chem. Soc. Jpn.* **1965**, *38*, 1314–1318.

[31]. Fowler, F. W.; Katritzky, A. R.; Rutherford, R. J. D. The correlation of solvent effects on physical and chemical properties. *J. Chem. Soc.* **1971**, 460–469.

[32]. Hammud, H. H.; Ghannoum, A. M.; Fares, F. A.; Abramian, L. K.; Bouhadir, K. H. New 1,6-heptadienes with pyrimidine bases attached: Syntheses and spectroscopic analyses. *J. Mol. Struct.* **2008**, *881*, 11–20.

[33]. Asuero, A. G.; Sayago, A.; González, A. G. The correlation coefficient: An overview. *Crit. Rev. Anal. Chem.* **2006**, *36*, 41–59.

[34]. Husain, M. M.; Sindhu, R.; Tandon, H. C. Photophysical properties and estimation of ground and excited state dipole moments of 7-diethylamino and 7-diethylamino-4-methyl coumarin dyes from absorption and emission spectra. *Eur. J. Chem.* **2012**, *3*, 87–93.

[35]. Masoud, M. S.; Ali, A. E.; Ghareeb, D. A.; Nasr, N. M. Spectroscopic behavior and equilibrium studies of some metallocephalosporins. *J. Mol. Liq.* **2016**, *224*, 914–929.

[36]. Masoud, M. S.; Hindawy, A. M.; Soayed, A. A.; El-Kaway, M. Y. A. Changes induced by solvent polarity in electronic absorption spectra of some nucleic acid constituents. *Fluid Phase Equilib.* **2011**, *312*, 37–59.

[37]. Zuleta, J. A.; Bevilacqua, J. M.; Eisenberg, R. Solvatochromic and emissive properties of pt(II) complexes with 1,1- and 1,2-ditholates. *Coord. Chem. Rev.* **1991**, *111*, 237–248.

[38]. Golchoubian, H.; Moayyedi, G.; Rezaee, E.; Bruno, G. Synthesis, characterization and solvatochromism study of mixed-chelate copper(II) complexes: A combined experimental and density functional theoretical study. *Polyhedron* **2015**, *96*, 71–78.

[39]. Abu-Eittah, R. H.; Khedr, M. K. The electronic absorption spectra of pyridine azides, solvent-solute interaction. *Spectrochim. Acta A Mol. Biomol. Spectrosc.* **2009**, *71*, 1688–1694.

[40]. Wang, P.; Anderko, A. Computation of dielectric constants of solvent mixtures and electrolyte solutions. *Fluid Phase Equilib.* **2001**, *186*, 103–122.

[41]. Laurence, C.; Nicolet, P.; Dalati, M. T.; Abboud, J.-L. M.; Notario, R. The empirical treatment of solvent-solute interactions: 15 years of .Pi. *J. Phys. Chem.* **1994**, *98*, 5807–5816.

[42]. Gálico, D. A.; Nova, C. V.; Guerra, R. B.; Bannach, G. Thermal and spectroscopic studies of the antioxidant food additive propyl gallate. *Food Chem.* **2015**, *182*, 89–94.

[43]. Osman, A.; Abu-Eittah, R. Complex formation between copper(II) and thiobarbiturates. *J. Pharm. Sci.* **1980**, *69*, 1164–1168.

[44]. Trišović, N.; Banjac, N.; Valentić, N.; Ušćumlić, G. Solvent effects on the structure-activity relationship of phenytoin-like anticonvulsant drugs. *J. Solution Chem.* **2009**, *38*, 199–208.

[45]. Sıdır, İ.; Taşal, E.; Gülseven, Y.; Güngör, T.; Berber, H.; Öğretir, C. Studies on solvatochromic behavior of some monoazo derivatives using electronic absorption spectra. *Int. J. Hydrogen Energy* **2009**, *34*, 5267–5273.

[46]. Ebead, Y. H.; Selim, M. A.; Ibrahim, S. A. Solvatochromic, acid-base features and time effect of some azo dyes derived from 1,3-benzothiazol-2-ylacetonitrile: experimental and semiempirical investigations. *Spectrochim. Acta A Mol. Biomol. Spectrosc.* **2010**, *75*, 760–768.

[47]. Chiappe, C.; Pieraccini, D. Ionic liquids: solvent properties and organic reactivity. *J. Phys. Org. Chem.* **2005**, *18*, 275–297.

[48]. Crowhurst, L.; Falcone, R.; Lancaster, N. L.; Llopis-Mestre, V.; Welton, T. Using Kamlet-Taft solvent descriptors to explain the reactivity of anionic nucleophiles in ionic liquids. *J. Org. Chem.* **2006**, *71*, 8847–8853.

[49]. Duereh, A.; Sato, Y.; Smith, R. L., Jr; Inomata, H. Analysis of the cybotactic region of two renewable lactone-water mixed-solvent systems that exhibit synergistic Kamlet-Taft basicity. *J. Phys. Chem. B* **2016**, *120*, 4467–4481.

[50]. Eto, M.; Tajiri, O.; Nakagawa, H.; Harano, K. Correlation of thione-to-thiol rearrangement rates of xanthates with solvent scales. Analysis of the reaction behavior by the Kamlet-Taft parameters, , α and β. *Tetrahedron* **1998**, *54*, 8009–8014.

[51]. Yazdanbakhsh, M. R.; Mohammadi, A. Synthesis, substituent effects and solvatochromic properties of some disperse azo dyes derived from N-phenyl-2, 2′-iminodiethanol. *J. Mol. Liq.* **2009**, *148*, 35–39.

[52]. Reichardt, C. Solvents and solvent effects: An introduction. *Org. Process Res. Dev.* **2007**, *11*, 105–113.